Design of an exoskeleton for strengthening the upper limb muscle for overextension injury prevention

Tzong-Ming Wu, Shu-Yi Wang, Dar-Zen Chen *

Dept. of Mechanical Engineering, National Taiwan University, Taipei, Taiwan, 10617

ARTICLE INFO

ABSTRACT

Several methods have been proposed for upper limb muscle training using exercise devices or machines to strengthen the muscle groups. However, most exercises control the direction of resistance to isolate specific muscle groups that need to be trained. A compact and cost-effective upper limb exoskeleton design with a 3-DOF shoulder joint and a 1-DOF elbow joint allows a patient or a healthy individual to move the limb in different planes and increases resistance through adjustments of the spring length to train more muscle groups. The exoskeleton springs were designed to equalize the joint torques for the shoulder and elbow joints with the joint torques obtained from free-weight exercises. Experimental data of the joint torques for two healthy subjects for shoulder abduction–adduction, flexion–extension, and elbow flexion–extension exercises with the exoskeleton were compared to measurements obtained from the upper limb dumbbell lateral raise, the dumbbell frontal raise, and the dumbbell curl exercises. The results of our preliminary evaluation showed that this design had an equivalent effect on the joint torques of shoulder and elbow to the free-weight exercises without the risk of overextension injury. Ultimately, this study provided a design and prototype for an upper limb exoskeleton.

© 2011 Elsevier Ltd. All rights reserved.

1. Introduction

The mechanical behavior of skeletal muscle contributes to the function and/or dysfunction of the human musculoskeletal system [1]. The muscle strength in an individual's limbs is crucial for physical independence. For example, in the upper limbs, impaired arm and hand function may cause serious limitations in daily living activities for the majority of stroke patients. In addition, whether older individuals have adequate muscle strength has a great influence on their daily living activities. Hisamoto and Higuchi [2] demonstrated that the extremity joint torque (EJT) values measured in 1000 healthy Japanese men and women aged between 20 and 70 showed that women in their 20s had significantly lower EJT values than women in their 40s or 50s in the upper limbs (i.e., wrist palmar flexion, wrist dorsiflexion, elbow flexion, elbow extension, and shoulder extension). One EJT value in the lower limbs (hip flexion) also differed. The results were attributed to the use of excessive automation and labor-saving equipment, which has diminished opportunities for muscle use in daily life.

Appropriate muscle training can not only enhance muscular strength, power, and endurance but also improve health and fitness by reinforcing cardiopulmonary function, reducing body fat, improving bone mineral density, and providing other benefits [3]. Resistance exercise leads to muscle hypertrophy and increased strength in both men and women, regardless of age. Decreased activity, on the other hand, produces a decrease in the cross-sectional area of muscle fibers and a loss of strength [1]. Resistance exercise has been widely adopted to help patients recover normal physiological functions after impairing motor activity and to improve dynamic stability [4,5]. The MIT-MANUS, a robot designed for clinical neurological application, was the first device to be evaluated extensively in clinical trials to examine whether robot-aided therapy was an acceptable form of exercise therapy for

stroke patients and whether it could improve the arm function of stroke patients [6]. Several studies on robotic devices have reported positive outcomes using various approaches, such as the MIME (mirror-image motion enabler) [7] and the ArmGuide [8].

Resistance exercises for fitness are often performed using fitness equipment. However, most conventional training devices use weights such as weight stacks combined with a training structure to provide resistance and accomplish training goals. For example, see U.S. patent 6394937 [9], U.S. patent 7601187 [10], and U.S. patent 7670269 [11]. A pulley system described in U.S. patent 6394937 couples a handle and weights in a single system. When the user exercises by manipulating the handle, the weight stack provides resistance and magnifies the effect of the exercise. U.S. patent 7235038 [12] is designed specifically for the elbow. However, the design is intended for exercising a single muscle group. Some machines use springs as a source of resistance (e.g., U.S. patent 5613928 [13] and U.S. patent 7060012 [14]). Most machines permit movements in a single plane to isolate specific muscle groups. These compare with free-weight exercises, where movement is allowed on different planes, training more muscle groups [3,15,16]. However, as the resistance increases, the inertial forces also increase, and the muscles have to produce more force to overcome the inertia of the heavier weights. This may cause a sports injury if the user operates the training devices improperly. The minimum resistance for this kind of training device is high, and these devices are more suitable for athletes than patients with muscle degeneration. A patient's training goals might not be accomplished using this type of training device, or the use of this kind of training device may cause an injury. The devices are also bulky, and the user has to travel to a gym or other location that has this type of training device, which could make the training more difficult to perform.

For these reasons, an upper limb training device that is able to perform arm exercises with multiple degrees of freedom would be beneficial to patients. In addition, it would be useful for the device to allow an individual to exercise or complete their physical therapy at a convenient time and to prevent injuries that could be caused by inertial forces. Such a device should be easy to adjust and carry, such that its use is not limited by space or location constraints.

In this study, we propose an unpowered upper limb exoskeleton design for use in strengthening the muscles of the upper limbs. The upper limb exoskeleton consists of a 3-DOF shoulder joint and a 1-DOF elbow joint. The upper arm can perform internal–external (int-ext), abduction–adduction (abd-add), and flexion–extension (flx-ext) motions. The forearm is also able to carry out a flexion–extension motion. The motion joint torques of the shoulder and elbow joints in the upper limb exoskeleton are equivalent to the objective joint torques obtained from models of free-weight exercise, such as the dumbbell lateral raise motion, dumbbell frontal raise motion, dumbbell curl motion, and overhead triceps extension. By altering the arrangement of low-inertia springs, the locations of the springs can be adjusted for higher intensity training, and the gravitational potential energies for the upper limb and the exoskeleton remain constant, which differs from free-weight exercises, where external weights are increased to induce large inertial changes for greater muscle strengthening. As such, the exoskeleton should be capable of preventing injuries that arise as the result of large inertial changes. The upper limb exoskeleton could be used for muscle strengthening or muscle strength recovery as it has the advantages of a compact and cost-effective design that is easy to operate and prevents injuries. These advantages make the exoskeleton very suitable for people or patients who can manipulate the active-resisted mode movement of the robotic devices for moderate exercise, and it can be used for home-based rehabilitation in the absence of a fitness instructor or therapist.

2. Kinematic model and joint torque analysis

2.1. Kinematic model of the upper limb

An upper limb includes the upper arm and forearm. The upper arm in Fig. 1 is pictured from the glenohumeral (GH) joint S to the elbow joint E, and the forearm extends from the elbow joint E to the middle of the palm of the hand H. The segmental lengths of the upper arm and the forearm are r_{SE} and r_{EH}, respectively. The hand is usually held in a neutral position during forearm movements. Therefore, the gravitational variation due to the wrist motion is negligible. Hence, the upper limb can be modeled as a two-link linkage. The geometries of the upper arm and the forearm were assumed to be axially symmetric, and the positions of the centers of mass, M_u and M_f, were assumed to be fixed and located at the center lines with respect to the upper arm and forearm. The mass of the human hand was ignored here as it is relatively light compared to the upper limb as a whole. The kinematic model for the arm linkage is shown in Fig. 1, and the GH joint in the human skeleton, which connects the scapular and the humerus, was modeled using a 3-DOF ball joint at point S. Kinematically, any Euler angle sequence of three orthogonal rotation axes can be used to model three pure rotations of the GH center point, including the shoulder internal–external rotation, abduction–adduction, and flexion–extension. The elbow joint is regarded as a revolute joint at point E, which provides only elbow flexion–extension.

When modeling the kinematic motion of the upper limb, we used the Denavit–Hertenberg (D-H) parameters for kinematic modeling of the upper limb. Following the conventions established by Denavit–Hertenberg and presented in Fig. 1, four Cartesian coordinate systems (CSs), CS 1, 2, 3, and 4, were attached to each link, and CS 0 was attached to the ground. The link parameters established between links i and $i-1$ are described based on the definition of D-H notation.

The inside portion of the human shoulder is called the shoulder girdle, and consists of a clavicle and scapular. Klopčar et al. [17] indicate that the girdle motion can be modeled using two degrees of freedom. In our study, the motion of the girdle was modeled using two parallelogram linkages and two serially connected links. The assembly is shown in the posterior linkage from Fig. 1. The parallelogram linkages provide the elevation–depression movement of the scapular, and the two serially connected links allowed the GH center to be free on the horizontal plane.
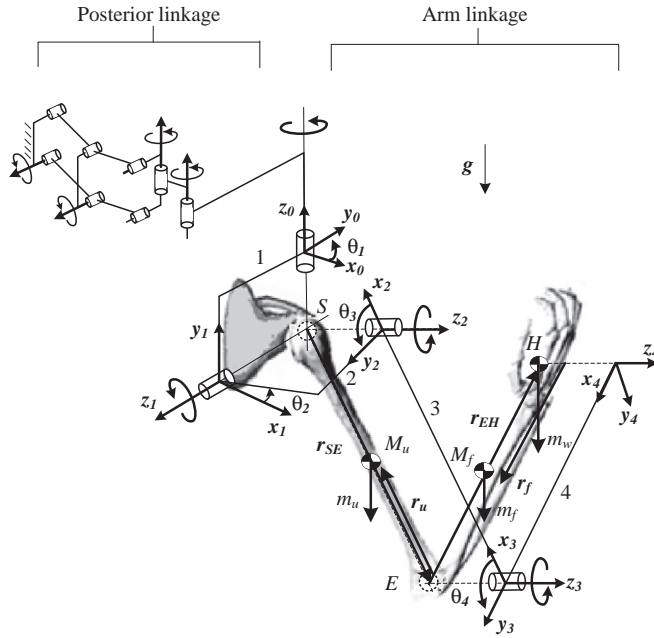
Fig. 1. Kinematic model and coordinate system of the right upper limb.

2.2. Static joint torques during free-weight exercise

Free-weight exercises are muscular exercises that use an external weight as a resistant force on a freely moving body. The muscle force is strengthened by increasing the free-weight load gradually. In Fig. 1, an objective model is constructed as a free-weight exercise using an external load m_w grasped in the middle of the palm H as well as the segmental masses of the upper arm and forearm. The values for m_u and m_f are located at the mass centers of the upper arm and the forearm, respectively. During exercise, the gravitational potential energy of the kinematic model can be expressed as

$$
\begin{aligned}
V_g = &\ -m_u\mathbf{g}\cdot(\mathbf{r_{SE}} + \mathbf{r_u}) - m_f\mathbf{g}\cdot(\mathbf{r_{SE}} + \mathbf{r_{EH}} + \mathbf{r_f}) - m_w\mathbf{g}\cdot(\mathbf{r_{SE}} + \mathbf{r_{EH}}) \\
= &\ -m_u(-\mathbf{g}\boldsymbol{k}_0)\cdot\left(-r_{SE}\boldsymbol{i}_3 + r_{u,x}\boldsymbol{i}_3\right) - m_f(-\mathbf{g}\boldsymbol{k}_0)\cdot\left(-r_{SE}\boldsymbol{i}_3 - r_{EH}\boldsymbol{i}_4 + r_{f,x}\boldsymbol{i}_4\right) \\
&\ -m_w(-\mathbf{g}\boldsymbol{k}_0)\cdot(-r_{SE}\boldsymbol{i}_3 - r_{EH}\boldsymbol{i}_4)
\end{aligned}
\tag{1}
$$

where r_u and r_f are the mass center position vectors of m_u and m_f referenced for each corresponding CS, and the quantities $r_{u,x}$, $r_{u,y}$, $r_{u,z}$, $r_{f,x}$, $r_{f,y}$, and $r_{f,z}$ are the corresponding local coordinates. Note that quantities $r_{u,y}$ and $r_{f,y}$ are omitted in Eq. (1). For CS 0, the quantities $r_{u,z}$ and $r_{f,z}$ are zero. The mass center of m_w was assumed to be located at point H.

Derived from the D-H transformation matrix and the parameters, Eq. (1) yields the following equation for the total gravitational potential energy of an objective model of free-weight exercise

$$
V_g = \left[-m_u g\left(r_{SE}-r_{u,x}\right)-\left(m_f + m_w\right)gr_{SE}\right]\sin\theta_2\cos\theta_3 - \left[m_f g\left(r_{EH}-r_{f,x}\right) + m_w gr_{EH}\right]\sin\theta_2\cos(\theta_3 + \theta_4)
\tag{2}
$$

In muscular exercise, external loads can produce points around the pivot joint where there is a tendency for the muscle to resist the opposite torques from external loads. Therefore, whether the muscle exercises or not can be learned from the changes in joint torques. The gravitational joint torque τ_i on the joint i is calculated as

$$
\tau_i = \frac{\partial V}{\partial \theta_i} \quad i = 1, 2, 3, 4
\tag{3}
$$

Eq. (3) suggests that the joint torque of θ_1 is zero and the joint torques of θ_2, θ_3 and θ_4 are τ_2, τ_3 and τ_4. The gravitational joint torques of the upper limb for the free-weight exercise are derived as

$$
\tau_2 = \left[-m_u g\left(r_{SE}-r_{u,x}\right)-\left(m_f + m_w\right)gr_{SE}\right]\cos\theta_2\cos\theta_3 - \left[m_f g\left(r_{EH}-r_{f,x}\right) + m_w gr_{EH}\right]\cos\theta_2\cos(\theta_3 + \theta_4)
\tag{4}
$$

$$
\tau_3 = \left[m_u g\left(r_{SE}-r_{u,x}\right) + \left(m_f + m_w\right)gr_{SE}\right]\sin\theta_2\sin\theta_3 + \left[m_f g\left(r_{EH}-r_{f,x}\right) + m_w gr_{EH}\right]\sin\theta_2\sin(\theta_3 + \theta_4)
\tag{5}
$$

$$\tau_4 = \left[m_f g \left(r_{EH} - r_{f,x} \right) + m_w g r_{EH} \right] \sin \theta_2 \sin(\theta_3 + \theta_4). \tag{6}$$

3. Conceptual design of the spring-loaded exoskeleton

3.1. Upper limb exoskeleton

In Fig. 1, the upper limb exoskeleton was separated from the arm linkage and posterior linkage. The posterior linkage was achieved through parallelogram linkages for girdle motions. In this study, only the arm linkage was taken into account in the design. In practice, using the exoskeleton configuration shown in Fig. 1, Links 1 and 2 interfere with the posterior side of the human body when the upper limb is rotated outward horizontally. The GH joint is comprised of the three revolute joint axes z_0, z_1 and z_2, which are arranged to be orthogonal to each other. However, this design is difficult to produce due to the difficulty of designing the human GH joint center. As such, we present a modified design in Fig. 2 that avoids these drawbacks, and the exoskeleton becomes wearable using a band on the upper arm and a handle for gripping.

The modified exoskeleton configuration shown in Fig. 2 was constructed using four links, and the 4-DOF kinematic chain contains four links, where Link 1 and the posterior linkage are connected by a revolute joint at axis $z_0{}^*$. Links 1 and 2 are connected by the other revolute joint at axis $z_1{}^*$. The axes $z_0{}^*$ and $z_1{}^*$ are parallel to axes z_0 and z_1, respectively, and the rotational joint angles for the $z_0{}^*$ and $z_1{}^*$ axes are the same as the rotational angles for the shoulder int-ext and abd-add exercises (θ_1 and θ_2). Links 2 and 3 pivot using a revolute joint at axis z_2, and the rotational joint angle near axis z_2 is θ_3. The interference problem arising between Link 1 and the human body was resolved by parallel shifting the axis of the shoulder int-ext, and the 3-DOF shoulder joint yielded three revolute joints near axes $z_0{}^*$, $z_1{}^*$ and z_2, where only the alignment of the z_2-axis and the human GH joint center is required. The point P is the intersection of axes $z_1{}^*$ and z_2, and the measurements taken near point P are the same as those at the human shoulder joint S. For the 1-DOF elbow joint, Links 3 and 4 pivot using a revolute joint at axis z_3 to accomplish the elbow flx-ext exercise. CSs 0, 1, 2, 3, and 4 are used in the modified exoskeleton configuration, and the relationships between the four CSs are the same as those shown in the previous analysis (Fig. 1).

By taking the link masses of the exoskeleton into account, the gravitational potential energy of Links 1, 2, 3, and 4 can be derived using the following equations:

$$V_{L1} = -m_1 \mathbf{g} \cdot \mathbf{r}_1 = const. \tag{7}$$

$$V_{L2} = -m_2 \mathbf{g} \cdot \mathbf{r}_2 = m_2 g r_{2,x} \sin\theta_2 - m_2 g r_{2,z} \cos\theta_2 + const. \tag{8}$$

$$V_{L3} = -m_3 \mathbf{g} \cdot \mathbf{r}_3 = m_3 g \left(r_{3,x} - r_{SE} \right) \sin \theta_2 \cos\theta_3 - m_3 g r_{3,z} \cos\theta_2 + const. \tag{9}$$

$$V_{L4} = -m_4 \mathbf{g} \cdot \mathbf{r}_4 = -m_4 g r_{SE} \sin \theta_2 \cos\theta_3 + m_4 g \left(r_{4,x} - r_{EH} \right) \sin\theta_2 \cos(\theta_3 + \theta_4) - m_4 g r_{4,z} \cos\theta_2 + const. \tag{10}$$

Here, m_i is the mass of link i of the exoskeleton; $r_{i,x}$, $r_{i,y}$, and $r_{i,z}$ describe their corresponding coordinates for the mass center of the link i on local coordinate x_i-y_i-z_i; and i is 1, 2, 3, and 4. It is assumed that Links 3 and 4 are axis-symmetrical links. Therefore, $r_{3,y}$ and $r_{4,y}$ are negligible.
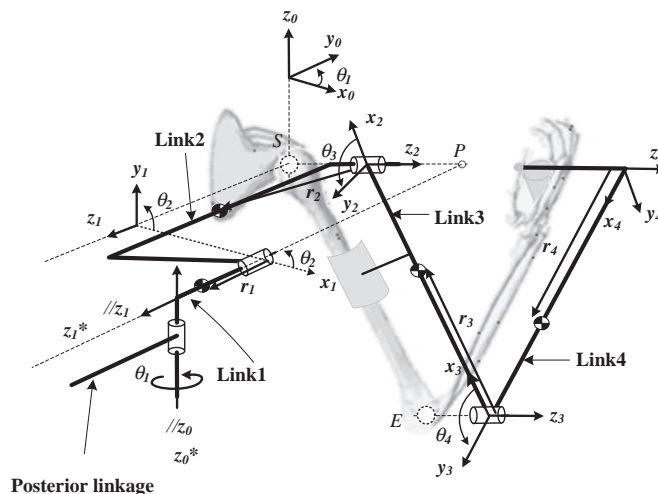
Fig. 2. A modified exoskeleton configuration.

Instead of using external loads, an increase in the amount of resistant force from the upper limb exoskeleton is achieved by changing the elastic force of the loaded spring. The resistance can be changed by adjusting the locations of the spring connections. On the spring-loaded exoskeleton, spring K_1 was attached to Point *A1* on Link 2 and Point *B1* on Link 1; Spring K_2 was attached to Point *A2* on Link 2 and Point *B2* on Link 4; and Spring K_3 was attached to Point *A3* on Link 2 and Point *B3* on Link 4. The location of the connected Points *A1*, *A2*, and *A3* for Springs K_1, K_2, and K_3 were adjusted for increased spring resistance, whereas Points *B1*, *B2*, and *B3* were fixed to connected points. The schematic diagram of the spring-loaded exoskeleton is shown in Fig. 3.

The concept of employing elastic force as a resistance force originated from the reverse idea behind the gravity-balance mechanism. The zero-free-length spring is used to make the spring stiffness independent of the rotational angles of the links. Therefore, the resistance force can be changed only by adjusting the locations of the spring connections. The design of zero-free-length springs was adopted in the spring-loaded exoskeleton, and this was accomplished by combining the use of standard springs with cables, and pulleys or alignment shafts [18,19].

The corresponding elastic potential energies, V_{S1}, V_{S2}, and V_{S3} of Springs K_1, K_2, and K_3 are derived as

$$
\begin{aligned}
V_{S1} &= \frac{1}{2}K_1(\boldsymbol{l}_{A1B1}\cdot\boldsymbol{l}_{A1B1}) \\
&= (-K_1 l_{CA1} l_{PB1})\sin\theta_2 - (K_1 l_{CP} l_{PB1})\cos\theta_2 + const.
\end{aligned}
\tag{11}
$$

$$
\begin{aligned}
V_{S2} &= \frac{1}{2}K_2(\boldsymbol{l}_{A2B2}\cdot\boldsymbol{l}_{A2B2}) \\
&= (-K_2 l_{SA2} r_{SE})\cos\theta_3 + (-K_2 l_{EB2} l_{SA2})\cos(\theta_3+\theta_4) + (K_2 r_{SE} l_{EB2})\cos\theta_4 + const.
\end{aligned}
\tag{12}
$$

$$
\begin{aligned}
V_{S3} &= \frac{1}{2}K_3(\boldsymbol{l}_{A3B3}\cdot\boldsymbol{l}_{A3B3}) \\
&= (K_3 l_{SA3} r_{SE})\cos\theta_3 - (K_3 l_{EB3} l_{SA3})\cos(\theta_3+\theta_4) - (K_3 l_{EB3} r_{SE})\cos\theta_4 + const.
\end{aligned}
\tag{13}
$$

The total potential energy of the upper limb exoskeleton is the sum of the gravitational energies of the upper limb and the four links with the elastic potential energies of the three springs.

Thus, using Eq. (3), the joint torques of θ_2, θ_3 and θ_4 from the use of the exoskeleton are M_2, M_3 and M_4, and the torques are derived as

$$
\begin{aligned}
M_2 &= \Big[-m_u g\big(r_{SE}-r_{u,x}\big) - m_f g r_{SE} + m_3 g\big(r_{3,x}-r_{SE}\big) - m_4 g r_{SE}\Big]\cos\theta_2\cos\theta_3 + \Big[-m_f g\big(r_{EH}-r_{f,x}\big) + m_4 g\big(r_{4,x}-r_{EH}\big)\Big]\cos\theta_2\cos(\theta_3+\theta_4) \\
&\quad + \Big[-K_1 l_{CA1} l_{PB1} + m_2 g r_{2,x}\Big]\cos\theta_2 + \Big[K_1 l_{CP} l_{PB1} + m_u g r_{u,z} + m_f g r_{f,z} + m_2 g r_{2,z} + m_3 g r_{3,z} + m_4 g r_{4,z}\Big]\sin\theta_2
\end{aligned}
\tag{14}
$$

$$
\begin{aligned}
M_3 &= \Big[m_u g\big(r_{SE}-r_{u,x}\big) + m_f g r_{SE} - m_3 g\big(r_{3,x}-r_{SE}\big) + m_4 g r_{SE}\Big]\sin\theta_2\sin\theta_3 + \Big[m_f g\big(r_{EH}-r_{f,x}\big) - m_4 g\big(r_{4,x}-r_{EH}\big)\Big]\sin\theta_2\sin(\theta_3+\theta_4) \\
&\quad + [K_2 l_{SA2} r_{SE} - K_3 l_{SA3} r_{SE}]\sin\theta_3 + [K_2 l_{EB2} l_{SA2} + K_3 l_{EB3} l_{SA3}]\sin(\theta_3+\theta_4)
\end{aligned}
\tag{15}
$$

$$
M_4 = \Big[m_f g\big(r_{EH}-r_{f,x}\big) - m_4 g\big(r_{4,x}-r_{EH}\big)\Big]\sin\theta_2\sin(\theta_3+\theta_4) + [K_2 l_{EB2} l_{SA2} + K_3 l_{EB3} l_{SA3}]\sin(\theta_3+\theta_4) - [K_2 l_{EB2} r_{SE} - K_3 l_{EB3} r_{SE}]\sin\theta_4
\tag{16}
$$
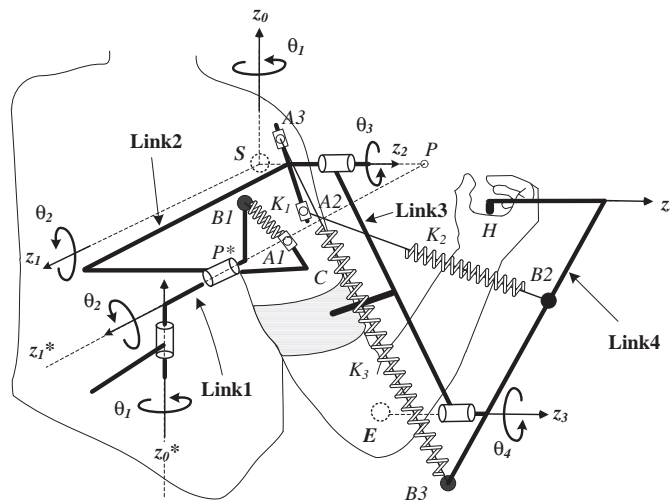
Fig. 3. A schematic diagram of the spring-loaded exoskeleton.

3.2. Spring design constrains for upper limb muscular exercise

The 3 DOF motions of the shoulder: shoulder int-ext, shoulder abd-add, and shoulder flx-ext have a wider range of movement than the dumbbell bench fly, the dumbbell lateral, and the frontal raise motions of free-weight exercises. The dumbbell bench fly is an exercise where the user lies on a bench and gravity acts in the direction of negative y_0 for CS 0 to provide torque on the shoulder joint near the axis of the shoulder int-ext motion. However, in this study, the stand posture was the position where gravity acts in the direction of negative k_o for CS 0. This makes the torque of shoulder int-ext motion zero. Therefore, only the dumbbell lateral and frontal raise motions for shoulder abd-add and flx-ext exercises for the shoulder joint, and dumbbell curl motion and overhead triceps extension for elbow flx-ext exercises for the elbow joint were taken into account for the upper limb exoskeleton, as shown in Fig. 4.

3.2.1. Training upper limb muscles with shoulder abduction/adduction

As an example of shoulder abd-add resistance exercise, the lateral raise motion was used for strengthening the deltoid, latissimus dorsi, pectoralis major, supraspinatus, and trapezius muscles [20]. In the kinematic model, the angles θ_3 and θ_4 were fixed at 0 degrees. As such, the upper arm and forearm can be considered a single link, and the rotation about axis z_1 applies for θ_2 alone. By substituting the 0 degree condition for Angles θ_3 and θ_4 into Eqs. (4)–(6), the joint torques of θ_3 and θ_4 equal zero, and the joint torque of θ_2 is expressed as

$$\tau_{2,\,lr} = \left[-m_u g \left(r_{SE} - r_{u,x} \right) - m_f g \left(r_{SE} + r_{EH} - r_{f,x} \right) - m_w g (r_{SE} + r_{EH}) \right] \cos\theta_2 \tag{17}$$

In Fig. 3, Spring K_1 connects Link 1 and Link 2 to generate torques near the axis of shoulder abd-add. In this exercise, the upper limb maintains the same posture as the lateral raise motion with exoskeleton, except that the resistance from the external load is replaced using springs. The joint torques of a shoulder with the exoskeleton are obtained by substituting the same angles for the lateral raise motion (θ_3 and θ_4) into Eqs. (14)–(16). The joint torques of θ_3 and θ_4 are zero, the same values as those for the lateral raise motion. The joint torque of θ_2 can be calculated as

$$\begin{aligned} M_{2,\,lr} = &[-m_u g \left(r_{SE} - r_{u,x} \right) - m_f g \left(r_{SE} + r_{EH} - r_{f,x} \right) + m_2 g r_{2,x} + m_3 g \left(r_{3,x} - r_{SE} \right) \\ &+ m_4 g \left(r_{4,x} - r_{EH} - r_{SE} \right) - K_1 l_{CA1} l_{PB1}] \cos\theta_2 \\ &+ \left[K_1 l_{CP} l_{PB1} + m_u g r_{u,z} + m_f g r_{f,z} + m_2 g r_{2,z} + m_3 g r_{3,z} + m_4 g r_{4,z} \right] \sin\theta_2 \end{aligned} \tag{18}$$

For emulating free-weight exercise, the joint torques in the lateral raise motion and the upper limb exoskeleton should be equivalent to each other. As a result, the coefficients of $\cos\theta_2$ in Eq. (17) have to be equal to those in Eq. (18), and the coefficients

Shoulder abd-add exercise	Shoulder flx-ext exercise	Elbow flx-ext exercise

Lateral raise motion	Frontal raise motion	Dumbbell curl motion	Overhead triceps extension
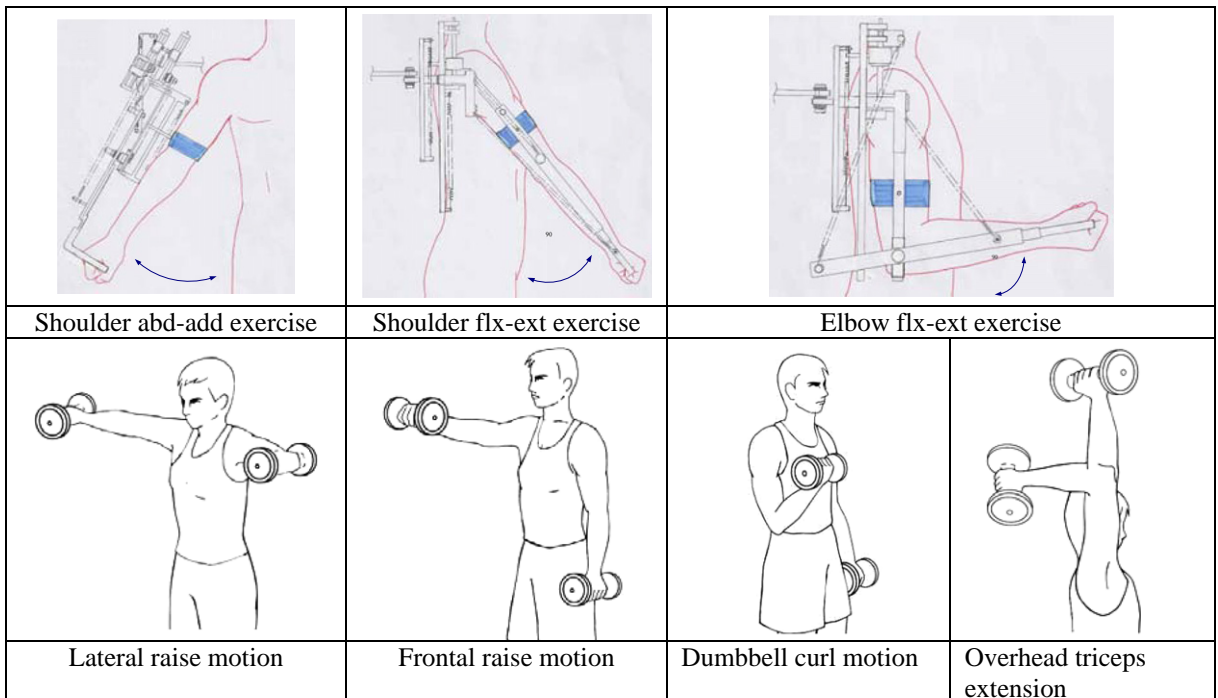
Fig. 4. Upper limb exoskeleton muscular exercise and dumbbell motions.

$sin\theta_2$ of Eq. (18) are zero. The design constrain of Spring K_1 obtained from the equation of coefficients with $cos\theta_2$ as expressed as

$$l_{CA1} = m_w \left[\frac{g(r_{SE} + r_{EH})}{K_1 l_{PB1}} \right] + \frac{m_2 g r_{2,x} + m_3 g \left(r_{3,x} - r_{SE} \right) + m_4 g \left(r_{4,x} - r_{EH} - r_{SE} \right)}{K_1 l_{PB1}} \tag{19}$$

Eq. (19) represents the linear proportion relationship between the weight of an external load m_w and the length of the connected points for Spring K_1, with an adjustment of l_{CA1} to increase the resistance for training intensity.

The weights of the upper limb and the exoskeleton generated momentum about axis z_1^* due to the effect of gravity, and Spring K_1 also compensated for the gravitational potential energy of the upper limb and the links. The spring design constrain of Spring K_1 is expressed as

$$l_{CP} = -\frac{m_u g r_{u,z} + m_f g r_{f,z} + m_2 g r_{2,z} + m_3 g r_{3,z} + m_4 g r_{4,z}}{K_1 l_{PB1}} \tag{20}$$

3.2.2. Training upper limb muscles with shoulder flexion/extension

As an example of shoulder flx-ext resistance exercise, the frontal raise motion can be used for strengthening deltoid, pectoralis major, latissimus dorsi, and trapezius muscles [20]. In the kinematic model, the angles θ_2 and θ_4 are fixed at 90 and 0 degrees, respectively. The upper arm and forearm are considered as a single rigid body rotating about axis z_2 with the angle θ_3. By substituting the conditions for θ_2 and θ_4 into Eqs. (4)–(6), the joint torque of θ_2 is equal to zero, and the joint torques of θ_3 and θ_4 can be expressed as

$$\tau_{3,fr} = \left[m_u g \left(r_{SE} - r_{u,x} \right) + m_f g \left(r_{SE} + r_{EH} - r_{f,x} \right) + m_w g (r_{SE} + r_{EH}) \right] \sin \theta_3 \tag{21}$$

$$\tau_{4,fr} = \left(m_f g \left(r_{EH} - r_{f,x} \right) + m_w g r_{EH} \right) \sin \theta_3 \tag{22}$$

In the frontal raise motion, the shoulder and elbow joints generate torques. Fig. 3 demonstrates that Spring K_2 connects Links 2 and 4, which produced torques that had the same strength as the same muscles using a free-weight exercise. For shoulder flx-ext exercise using the upper limb exoskeleton, a user would have the same movement as for the frontal raise motion. By substituting the same angles, θ_2 and θ_4, for frontal raise motion in Eqs. (14)–(16), the joint torques of the shoulder with the exoskeleton are obtained using the equations:

$$M_{2,fr} = K_1 l_{CP} l_{PB1} + m_u g r_{u,z} + m_f g r_{f,z} + m_2 g r_{2,z} + m_3 g r_{3,z} + m_4 g r_{4,z} \tag{23}$$

$$M_{3,fr} = \left[m_u g \left(r_{SE} - r_{u,x} \right) + m_f g \left(r_{SE} + r_{EH} - r_{f,x} \right) - m_3 g \left(r_{3,x} - r_{SE} \right) - m_4 g \left(r_{4,x} - r_{EH} - r_{SE} \right) + K_2 l_{SA2} (r_{SE} + l_{EB2}) + K_3 l_{SA3} (l_{EB3} - r_{SE}) \right] \sin \theta_3 \tag{24}$$

$$M_{4,fr} = \left[m_f g \left(r_{EH} - r_{f,x} \right) - m_4 g \left(r_{4,x} - r_{EH} \right) + K_2 l_{EB2} l_{SA2} + K_3 l_{EB3} l_{SA2} \right] \sin \theta_3 \tag{25}$$

To achieve the effects of frontal raise motion, the joint torques with the upper limb exoskeleton had to be the same as the joint torques for frontal raise motion. The design constrains for Springs K_2 and K_3 are calculated as

$$l_{EB3} = 0 \tag{26}$$

$$l_{EB2} = r_{EH} \tag{27}$$

$$l_{SA3} = \frac{-m_3 g r_{EH} \left(r_{3,x} - r_{SE} \right) + m_4 g r_{SE} r_{4,x}}{K_3 r_{SE} r_{EH}} \tag{28}$$

$$l_{SA2} = m_w \left(\frac{g}{K_2} \right) + \frac{m_4 g \left(r_{4,x} - r_{EH} \right)}{K_2 r_{EH}} \tag{29}$$

During shoulder flx-ext exercise, Spring K_1 could be installed in any position, and the spring position did not affect the results of the muscle strengthening exercises. The momentum about the axis z_1^* due to the weights of the upper limb and the links in the exoskeleton was the same as the momentum in shoulder abd-add exercise. Therefore, the design for Spring K_1 could be modelled using the same equations as presented in Eq. (20). Eq. (29) also represents a linear proportion between the weight of external load m_w and the length of the connected points of Spring K_2 with an adjustment l_{SA2} to increase the resistance for training intensity.

3.2.3. Training upper limb muscles with elbow flexion/extension

As an example of elbow flx-ext resistance exercise, the dumbbell curl motion is used for strengthening the biceps brachii, brachialis, and brachioradialis muscles. In addition, the overhead triceps extension is used for strengthening the triceps brachii [20]. In the kinematic model, the angles θ_2 and θ_3 were fixed at 90 and 0 degrees, respectively. The forearm rotates about axis z_3 with θ_4. Substituting the angles θ_2 and θ_3 into Eqs. (4)–(6) produced a joint torque for θ_2 of zero, whereas the joint torques for θ_3 and θ_4 were equalized and expressed as

$$\tau_{3,dc} = \tau_{4,dc} = \left(m_f g \left(r_{EH} - r_{f,x} \right) + m_w g r_{EH} \right) \sin \theta_4 \tag{30}$$

In the dumbbell curl motion, the joint torques were generated on the joints of Axes z_3 and z_4, and the installation of Spring K_3 connected Link 2 and Link 4 to produce the same joint torques as for free-weight exercise (Fig. 3). For training the upper limb exoskeleton for the elbow flx-ext exercise, substituting the angles θ_2 and θ_3 for the dumbbell curl motion into Eqs. (4)–(6) and (14)–(16) yielded the joint torques for the upper limb exoskeleton. The joint torque of θ_2 are the same as the shoulder flx-ext exercise expressed using Eq. (30), whereas the joint torques for θ_3 and θ_4 are

$$M_{3,dc} = \left[m_f g \left(r_{EH} - r_{f,x} \right) - m_4 g \left(r_{4,x} - r_{EH} \right) + K_2 l_{EB2} l_{SA2} + K_3 l_{EB3} l_{SA3} \right] \sin \theta_4 \tag{31}$$

$$M_{4,dc} = \left[m_f g \left(r_{EH} - r_{f,x} \right) - m_4 g \left(r_{4,x} - r_{EH} \right) + K_2 l_{EB2} l_{SA2} + K_3 l_{EB3} l_{SA3} - K_2 l_{EA2} r_{SE} + K_3 l_{EB3} r_{SE} \right] \sin \theta_4 \tag{32}$$

The joint torques for θ_3 and θ_4 for the upper limb exoskeleton have to be to the same as for the dumbbell curl motion. As such, the design constrains for Springs K_2 and K_3 are expressed as

$$l_{EB2} = \frac{K_3 l_{EB3}}{K_2} \tag{33}$$

$$l_{SA2} = 0 \tag{34}$$

$$l_{SA3} = m_w \left(\frac{g r_{EH}}{K_3 l_{EB3}} \right) + \frac{m_4 g \left(r_{4,x} - r_{EH} \right)}{K_3 l_{EB3}} \tag{35}$$

For the dumbbell curl motion, the increase in resistance is produced by increasing the weight of external load, m_w. However, due to the linear proportion relationship between m_w and K_3, the adjustment for Spring K_3, l_{SA3}, was used to increase the resistant force from Eq. (35) for training with the exoskeleton. The spring design constrain for Spring K_1 was the same as that for the lateral raise motion (see Eq. (20)).

The overhead triceps extension is a free-weight exercise that can be used to strengthen the triceps. In exercising with the upper limb exoskeleton, the motion can also be performed with the elbow flx-ext exercise. In the kinematic model, the angles θ_2 and θ_3 were fixed at 90 and 180 degrees, respectively, and the forearm was rotated about Axis z_3 with θ_4. By substituting the angles θ_2 and θ_3 into Eqs. (10)–(12) and (14)–(16), the joint torques can be calculated. The momentums for the free-weight exercise has to be the same as that for the upper limb exoskeleton. Therefore, the design constrains for Springs K_2 and K_3 were the same as those for the elbow flx-ext exercise for training biceps, as shown in Eqs. (33)–(35). In the elbow flx-ext exercise for training the biceps and triceps, Spring K_1 could be set to any position because it would not affect muscle strengthening.

4. Embodiment design and the prototype for the upper limb exoskeleton

The preliminary embodiment design was carried out using 3D CAD software, and the major materials for the links were made of aluminum alloy in this study. The material characteristics of the links were defined in the CAD software to determine the inertia parameters of the upper limb exoskeleton. The masses and the corresponding coordinates of the mass centers for each link are listed in Table 1.

The resistance in the design is generated by adjusting the locations of the springs rather than changing the stiffness of the springs. This design was expected to provide different levels of resistance to stimulate muscle strength recovery in patients with

Table 1
Inertial parameters of the upper limb exoskeleton.

Links (i)	Mass (kg)	$r_i x$ (mm)	$r_i y$ (mm)	$r_i z$ (mm)
1	0.949	−45	82	25
2	3.470	−13	29	−18
3	0.716	143	0	−75.4
4	0.867	94	0	−50.6

injuries and to provide more intense strength training for healthy individuals. In this study, the maximum resistant force was designed to be 49 N (corresponding to a 5 kg weight dumbbell). Therefore, it was important to choose springs of suitable stiffness. In the preliminary conceptual design of the upper limb exoskeleton, interference among the different links during exercise needed to be considered. For example, the attached point $B3$ was a prominent link on Link 4 that exceeded the elbow joint. In the upper limb stretching course, the motion interference of Link 4 and Link 2 would interfere if the length of the prominent link was longer than the upper arm. Therefore, l_{EB3} was designed to be 150 mm (i.e., shorter than the length of the subject's upper arm). The spring-adjustable points were limited from 1 mm to 160 mm. The adjustable lengths l_{CA1}, l_{SA2}, and l_{SA3} of Springs K_1, K_2 and K_3 were designed to be attached to Link 2, which was a reasonable and convenient location for setting the adjustment of the exoskeleton. Moreover, the length l_{B1P^*} was designed to be 155 mm, which conformed to the limitations of the adjustable range. Considering the limitations and the mass properties of the linkages, together with the anthropometric parameters of humans as expressed in Eq. (19), the range of spring stiffness for K_1 lies in the range

$$0.95 N / mm \leq K_1 \leq 1.51 N / mm \tag{36}$$

Following the same steps for the shoulder flx-ext exercise, the range of spring stiffness for K_2 was derived from Eq. (29), and for the elbow flx-ext exercise, the range of spring stiffness for K_3 was obtained from Eq. (35). The ranges of spring stiffness for K_2 and K_3 were

$$0.46 N / mm \leq K_2 \leq 1.36 N / mm \tag{37}$$

$$0.66 N / mm \leq K_3 \leq 3.27 N / mm \tag{38}$$

The K_1, K_2 and K_3 springs that were available within the stiffness ranges were selected for this design. During the practical implementation of this design, we chose springs with the following stiffness from the catalog [22] of standard springs: K_1 (1.421 N/mm (0.145 kgw/mm)), K_2 (0.49 N/mm (0.05 kgw/mm)) and K_3 (0.69 N/mm (0.07 kgw/mm)). The link lengths r_{SE} and r_{EH} of the upper arm and forearm could be measured based on an anthropometric database. According to the anthropometric resource from the Naval Biodynamics Laboratory [23], Chandler et al. [24], and the institute of occupational safety and health in Taiwan [25], the link lengths of upper arm and forearm, and the total body weight for small, medium, and large-sized human beings are listed in Table 2.

The spring design parameters of the exoskeleton were functions of the lengths of the upper arm and forearm and of the mass properties of the links. Using the values for m_u, m_f, r_{SE}, r_{EH}, K_1, K_2, and K_3, together with the link parameters, we calculated the range of spring-adjustable points, and these are listed in Table 3.

In the embodiment design for the device, the arrangement of three revolute joints for the 3-DOF shoulder joint is illustrated in Fig. 5(a). The revolute joints for Axes z_0, z_1, and z_2 were achieved using thrust bearings to decrease clearance defects. The elbow joint was accommodated using a revolute joint and selective connection positions for small, medium, and large-sized human beings to adjust the length of the upper limb for different subjects. Thrust bearings were used to achieve elbow flexion–extension motion. The length of the forearm link was also adjusted using a linear slide so that the device would fit different individuals. The CAD drawing is shown in Fig. 5(b).

Table 2
Anthropometric parameters of the upper limb.

Dimension descriptions	Small	Medium	Large
Upper arm (r_{SE}, mm)	224	255	286
Forearm (r_{EH}, mm)	267	317	368
Total body weight (TBW, kg)	44.3	62.1	79.9

Table 3
Detailed spring design parameters for the exoskeleton.

	Spring design parameters (mm) (Resistance:1 kg–5 kg)			
	Spring adjustments	Small	Medium	Large
Shoulder abd-add exercise	l_{CA1}	1–150	1–150	1–150
	l_{PB1}	155	155	155
Shoulder flx-ext exercise	l_{SA2}	7–90	7–90	7–90
	l_{EB2}	267	317	368
	l_{SA3}	8	8	8
	l_{EB3}	0	0	0
Elbow flx-ext exercise	l_{SA2}	0	0	0
	l_{EB2}	210	210	210
	l_{SA3}	11–160	11–160	11–160
	l_{EB3}	150	150	150
All exercises	l_{CP}	9	9	9

In this design, a standard spring with a wire and pulley construction was used to emulate a zero-free-length spring. The zero-free-length Spring K_1 was attached to Point *A1* on Link 1, and Point *A1* was attached to Link 2. An embodiment design of Spring K_1 was illustrated in Fig. 5(c), and the standard Spring K_1 was fixed using a pin and connected Point *B1* and Point *A1* with wire and pulleys. The distance of Point *B1* to *A1* was not limited to the free length of the spring. The arrangements for the K_2 and K_3 springs were the same as for Spring K_1 and are shown in Fig. 5(d). To increase the intensity of the exercise, the installation in Link 2 could be adjusted using three lead screws. The possibility of interference between the links and springs during exercise was carefully considered and eliminated during 3D CAD drawing.

A detailed design of the upper limb exoskeleton based on the embodiment design was completed, and a prototype, shown in Fig. 6, was built for functional and performance evaluations.
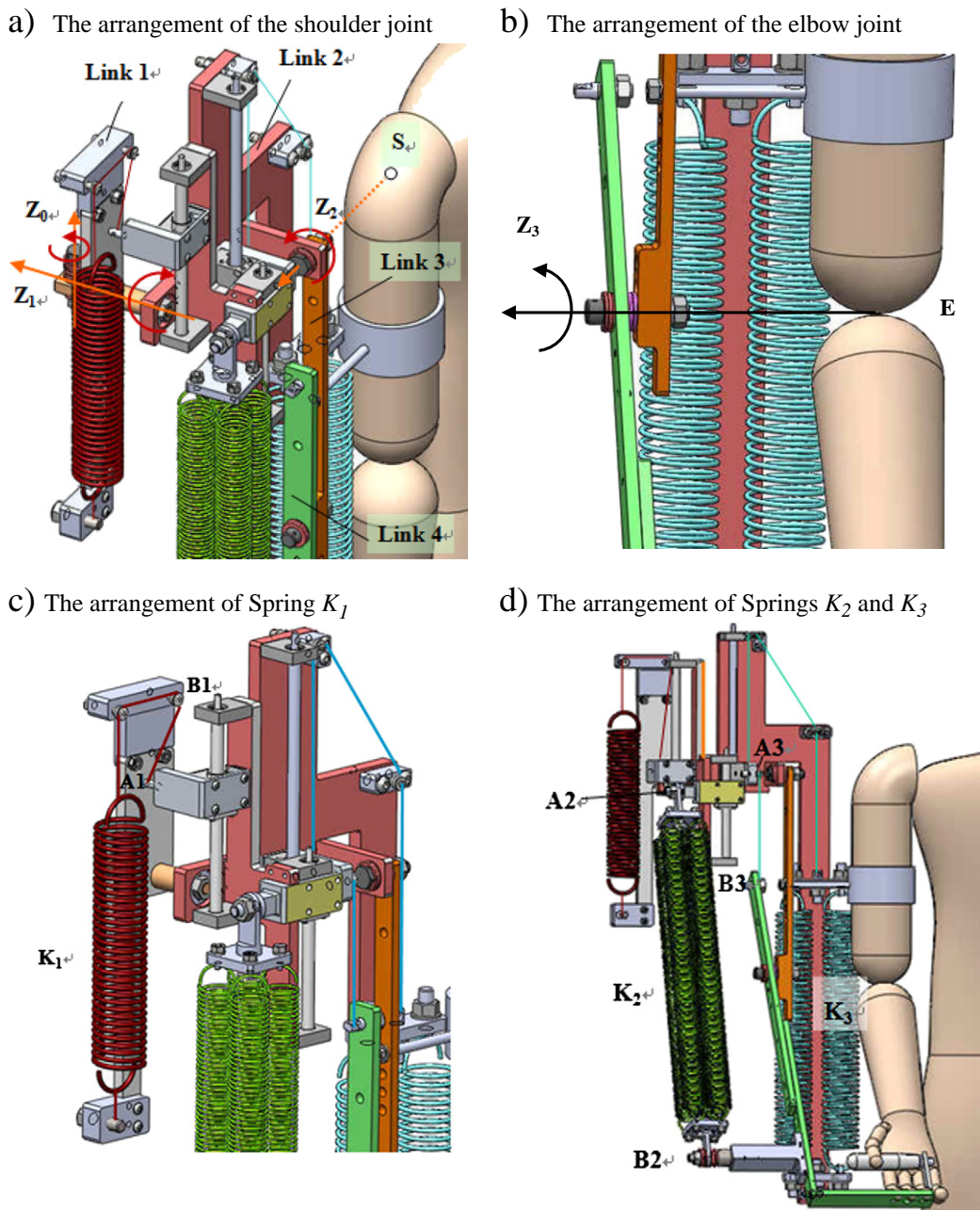
Fig. 5. Embodiment design of the upper limb exoskeleton.

Fig. 6. The perspective view of the prototype of upper limb exoskeleton.

5. Preliminary evaluation

5.1. Experimental set-up

Experimental study involved two healthy subjects, one male and one female, who volunteered to participate in this preliminary evaluation. Based on their self-reports, neither had any history of neural or musculoskeletal disease. Shoulder and elbow motions were recorded with a Vicon MX-F20 motion analysis system (Oxford Metrics, Ltd., Oxford, UK) at a capture rate of 100 Hz. This system utilized eight synchronized high-speed infrared charge-coupled display (CCD) cameras to track eight reflective markers, each 14 mm in diameter, mounted with double-sided hypoallergenic tape at the following bony anatomical landmarks on the subject's trunk and right upper limb: the seventh cervical vertebrae (C7), suprasternal notch (CLAV), acromion (RSHO), lateral epicondyle (RLEL), medial epicondyle (RMEL), processus styloideus radii (RMWR), processus styloideus ulnae (RLWR), and the metacarpophalangeal joint (MCP) of the right middle finger (RFIN). These maker locations were selected to best define the segments while minimizing skin motion.

An initial static calibration of the motion capture system, followed by a dynamic calibration, was performed before conducting this experiment. Motion capture software (Vicon Nexus 1.2) was used to digitize the body landmarks. After the markers were properly attached, the exoskeleton was mounted on an aluminum frame, and the joints of the exoskeleton were aligned with the subject's shoulder and elbow joints. While wearing the exoskeleton, the subjects were then asked to stand in the object-space, consisting of the field of view of the CCD cameras, and move their shoulders, elbows, and wrist joints to ensure that each marker could be captured by at least two cameras at all times during the data recording. The subjects then performed the selected free-weight exercise and shoulder abd-add, shoulder flx-ext, and elbow flx-ext movements in the object-space with the spring-loaded upper limb exoskeleton in place. The motion analysis system recorded each movement of the upper limb segment by tracking the

a) Shoulder flx-ext exercise with the upper limb exoskeleton

b) Shoulder abd-add exercise with the upper limb exoskeleton

c) Elbow flx-ext exercise with the upper limb exoskeleton
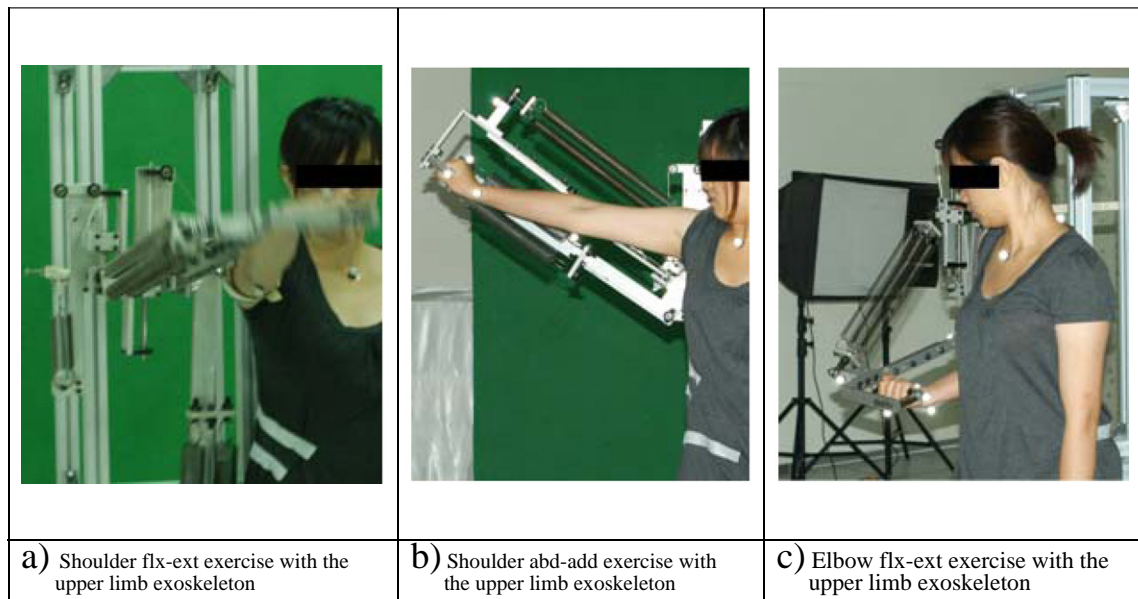
Fig. 7. Resistance exercises performed using the upper limb exoskeleton.

3-D location of the markers. Basic function tests consisted of an active range of motion, shoulder abd-add, shoulder flx-ext, and elbow flx-ext Vicon motion data were also collected for each subject (Fig. 7).

Table 4 shows the anthropometric parameters of the two healthy subjects, where TBW is the total body weight.

The resistant force was set at two different weight levels, 1 kg and 3 kg, for the free-weight exercise. The segmental weights for the upper arms and forearms are based on those given by DeLeva [21], who proposed the body segment parameter data estimation as shown below:

$$m_u = R_u \times (TBW) \tag{39}$$

$$m_f = R_f \times (TBW) \tag{40}$$

Here, R_u and R_f are the ratios of the weights of the upper arm and the forearm segments, respectively, as percentages of the total body weight; the ratios were 0.0271 and 0.0162 for the male subject and 0.0255 and 0.0138 for the female subject.

Based on the anthropometric parameters of the male and female subjects, the exact values of l_{CA1}, l_{SA2}, and l_{SA3} for the 1 kg and 3 kg weight resistances applied to the upper limb exoskeleton are listed in Table 5. The resistance was easily changed by adjusting

Table 4
Anthropometric parameters of the subjects.

Subjects	TBW	Upper arm (r_{SE})	Forearm (r_{EH})	Segmental weight (m_u)	Segmental weight (m_f)
Male	77 kg	280 mm	352 mm	2.09 kg	1.25 kg
Female	60 kg	263 mm	309 mm	1.53 kg	0.63 kg

Table 5
The adjustable length of springs for 1 and 3 kg weight resistances.

Subjects	Resistance (kg)	Adjustments of springs for muscle strengthening exercise (mm)		
		Shoulder abd-add (l_{CA1})	Shoulder flx-ext (l_{SA2})	Elbow flx-ext (l_{SA3})
Male	1	5	9	15
	3	74	49	82
Female	1	4	10	14
	3	67	50	73

the position of the nut of the leading screw corresponding to the selected exercise to a new position relative to the zero position (i.e., aligned with the Z_2 axis); these positions are listed Table 5.

5.2. Experimental protocols

Three common human movements were chosen for evaluation: shoulder add-abd, shoulder flx-ext, and elbow flx-ext. Each movement was performed in a slowly controlled manner for five consecutive repetitions: lifting (1 second) and then lowering (1 second), without sudden jerks or accelerations. The range of movement (90 degrees) in the evaluation was measured from the starting position (when the upper arm and forearm were pointing naturally downward) upward to the final position (when the upper arm and forearm, or just the forearm, were horizontal), and the direction was then reversed. To provide 1- and 3-kg and resistances in each case, dumbbells were used for the free-weight exercise, and the resistance was supplied by springs for the upper limb exoskeleton motion.
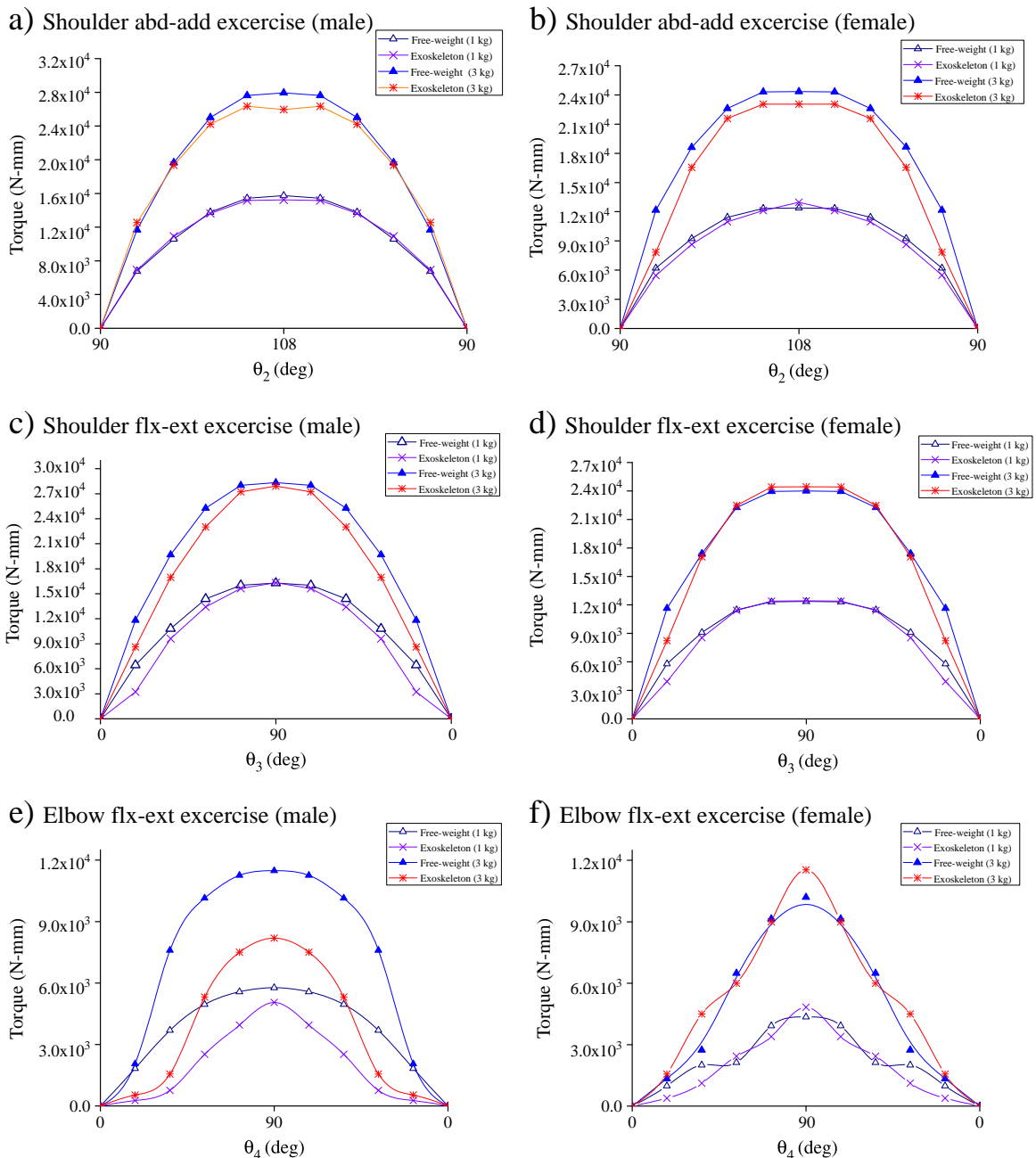
Fig. 8. Experimental data for joint torques with 1 kg and 3 kg resistances.

5.3. Data analysis

Detailed information was collected regarding the upper limb kinematics. The inverse dynamics approach is the most commonly used method for solving unknown reaction forces and moments. Joint torques were thus calculated using a 3D generic inverse dynamic method [26]. Motion analysis data for the exercises were obtained using the Vicon Nexus software. Analysis of the upper limb kinematics was restricted to the motion of the shoulder and elbow. The first three data sets for the five repeated trials were analyzed to obtain averaged results for the three sets; if one of these three data sets was unsuitable for data analysis, the fourth or the fifth data set was then substituted.

6. Results

Fig. 8 presents a comparison between the joint torques in the free-weight exercise and in the resistance exercise with the upper limb exoskeleton for these experiments. As shown in Fig. 8(a)–(d), the peak joint torques were at 180 degrees for the shoulder abd-add exercise and 90 degrees for the flx-ext exercise. The joints should generate higher torques when the upper limb is straightened in the horizontal position, where the moment arm has the greatest distance perpendicular to the resistant force for the joint. A similar reasoning can be applied to the elbow flx-ext exercise; the forearm is drawn upward in an arc from a vertical position to the horizontal position, whereas the forearm is pointing down to the vertical position in the reverse direction; this is illustrated in Fig. 8(e)–(f).

Based on the data collected from the preliminary evaluation, the tendencies observed for the shoulder add-abd, shoulder flx-ext, and elbow flx-ext resistance exercises with the upper limb exoskeleton were nearly equivalent to those for the joint torques obtained for the upper limb dumbbell lateral raise, the dumbbell frontal raise, and the dumbbell curl exercises (Fig. 8), which was expected. One exception was found in the elbow flx-ext exercise conducted by the female with 1 kg and 3 kg of resistance; by carefully examining the collected data, we found that differences arose in the movement of the shoulder joint of the exoskeleton during the elbow flx-ext exercise experiment. In the dumbbell curl motion, the upper arm must remain still, naturally pointing downward toward the ground. For consistency with the dumbbell curl motion, we suggest that the shoulder joint of the exoskeleton be held fixed when performing the elbow flx-ext exercise with the upper limb exoskeleton. The peak torques of the exercises and their differences are listed in Table 6.

7. Conclusions

We tested an unpowered upper limb exoskeleton designed for resistance exercise to strengthen the principal muscles of the upper limbs while preventing overextension injuries. A linear relationship was determined between the weight of the external load and the attached spring. Instead of changing the weight during the resistance exercise, the resistant force was provided by spring elements with moveable attachment points that could be adjusted to increase the intensity of muscular exercise. The upper limb exoskeleton was used to perform shoulder abduction–adduction, flexion–extension, and elbow flexion–extension exercises, and the torques of the shoulder and elbow joints with the exoskeleton were expected to be equal to the objective joint torques obtained from models of free-weight exercises. A prototype was constructed, and an on-line motion analysis was conducted to record designated motions by two subjects with free weights and with the upper limb exoskeleton. The data trends showed good conformity in all exercises, especially for the joint torque data in the shoulder add-abd and shoulder flx-ext exercises. Based on these preliminary results, this study provided a working prototype of a design for an upper limb exoskeleton with an adjustable upper arm and forearm length that is suitable for average-sized human beings. Because this device uses an arrangement of small inertial springs to provide resistance, it is capable of preventing the muscle injuries caused by large inertial forces.

Table 6
The peak torques and differences for the free-weight and upper limb exoskeleton exercises.

Subjects	Resistance (kg)	Free-weight $\bar{\tau}$ (N-mm)	Exoskeleton $\overline{M}$ (N-mm)	Difference (%)
Shoulder abd-add exercise				
Male	1	15,743	15,247	−3.15
	3	27,937	25,946	−7.12
Female	1	12,385	12,964	4.67
	3	24,344	23,049	−5.32
Shoulder flx-ext exercise				
Male	1	16,281	16,334	0.32
	3	28,326	27,925	−1.41
Female	1	12,366	12,440	0.59
	3	23,993	24,440	1.86
Elbow flx-ext exercise				
Male	1	5769	5054	−12.39
	3	11,485	8,193	−29.13
Female	1	4354	4827	10.86
	3	10,195	11,536	13.15

*$\bar{\tau}$: joint torques for the free-weight exercise; $\overline{M}$: joint torques for the exoskeleton exercise; D: $\overline{M} - \bar{\tau} / \bar{\tau} \times 100\%$.

Acknowledgment

References

[1] C.A. Oatis, Kinesiology: the mechanics & pathomechanics of human movement, second ed. Lippincott Williams & Wilkins, Baltimore, 2009.
[2] S. Hisamoto, M. Higuchi, Age-related changes in muscle strength of healthy Japanese, Standardization Center, NITE, Osaka, Japan, 2007 Human and Welfare Technology Division.
[3] C.J. Hass, M.S. Feigenbaum, B.A. Franklin, Prescription of resistance training for healthy populations, Sports Med. 31 (14) (2001) 953–964.
[4] L.F. Teixeira-Salmela, S.J. Olney, S. Nadeau, B. Brouwer, Muscle strengthening and physical conditioning to reduce impairment and disability in chronic stroke survivors, Arch. Phys. Med. Rehabil. 80 (10) (1999) 1211–1218.
[5] D.M. Scarborough, D.E. Krebs, B.A. Harris, Quadriceps muscle strength and dynamic stability in elderly persons, Gait & Posture 10 (1) (1999) 10–20.
[6] H.I. Kreb, N. Hogan, M.L. Aisen, B.T. Volpe, Robot-aided neurorehabilitation, IEEE Trans. Rehabil. Eng. 6 (1) (1998) 75–87.
[7] C.G. Burgar, P.S. Lum, P.C. Shor, H.F. Machiel Van der Loos, Development of robots for rehabilitation therapy: the Palo Alto VA/Stanford experience, J. Rehabil. Res. Dev. 37 (6) (2000) 663–673.
[8] D.J. Reinkensmeyer, L.E. Kahn, M. Averbuch, A. Mckenna-Cole, B.D. Schmit, W.Z. Rymer, Understanding and treating arm movement impairment after chronic brain injury: progress with the ARM guide, J. Rehabil. Res. Dev. 37 (6) (2000) 653–662.
[9] H.C. Voris, Handle and Exercise Arm Assembly for Use with Exercise Machine, U. S. Patent 6,394,937, May. 28, 2002.
[10] R.T. Webber, B. Hockridge, J.O. Meredith, Rigid Arm Pull Down Exercise Machine, U. S. Patent, 7601187 B2, Oct. 13, 2009.
[11] R.T. Webber, B. Hockridge, J.O. Meredith, Chest Press Exercise Machine with Self-Aligning Pivoting Upper Support, U. S. Patent 7670269 B2, Mar. 2, 2010.
[12] C.S. Liao, Arm Exerciser, U. S. Patent 7,235,038 B2, June 26, 2007.
[13] J.A. Laudone, Jointed Bar for an Exercise Machine, U. S. Patent, 5613928, Mar. 25, 1997.
[14] L.L. Howell, S.P. Magleby, Substantially Constant-Force Exercise Machine, U. S. Patent 7,060,012, Jun. 13, 2006.
[15] T.R. Baechle, R. Earle, Essentials of strength training and conditioning, human kinetics, National Strength & Conditioning Association, U.S., 2000.
[16] M.H. Stone, D. Collins, S. Plisk, G. Haff, M.E. Stone, Training principles: evaluation of modes and methods of resistance training, Strength Cond. J. 22 (3) (2000) 65–76.
[17] N. Klopčar, J. Lenarčič, Kinematic Model for Determination of Human Arm Reachable Workspace, Meccanica 40 (2) (2005) 203–219.
[18] S.K. Banala, S.K. Agrawal, A. Fattah, V. Krishnamoorthy, W.L. Hsu, J. Scholz, K. Rudlph, Gravity-Balancing Leg Orthosis and Its Performance Evaluation, IEEE Trans. Rob. 22 (6) (2006) 1228–1239.
[19] R. Barents, M. Schenk, W.D. Van Dorsser, B.M. Wisse, J.L. Herder, Spring-to-spring balancing as energy-free adjustment method in gravity equilibrators, Proc. ASME Int Des Eng Tech Conf Comput Inf Eng Inf. Eng. Conf. DETC **7** (part B), 2009, pp. 689–700.
[20] J. Hamill, K.M. Knutzen, Biomechanical basis of human movement, third ed. Lippincott Williams & Wilkins, Baltimore, 2009.
[21] P. DeLeva, Adjustments to Zatsiorsky-Seluyanov's Segment inertia parameters, J. Biomech. 29 (9) (1996) 1223–1230.
[22] The Stock Precision Engineered Components (SPEC), Associated Spring[Online]. Available: http://springming.so-buy.com/ezfiles/springming/img/img/61161/SPEC-04E.pdf.
[23] Naval Biodynamics Laboratory, Anthropometry and Mass Distribution for Human Analogues, Volume I: Military Male Aviators, Naval Medical Research and Development Command Bethesda, New Orleans, LA, 1988.
[24] R.F. Chandler, C.E. Clauser, J.T. McConville, H.M. Reynolds, J.W. Young, Investigation of inertial properties of the human body, Aerospace Medical Research Laboratory, Wright-Patterson AFB, Ohio, 1974 AFAMRL-TR-74-137.
[25] Institute of Occupational Safety & Health, 2008, [Online]. Available: http://www.iosh.gov.tw/Publish.aspx?cnid=26&P=812.
[26] R. Dumas, R. Aissaoui, J.A. De Guise, A 3D generic inverse dynamic method using wrench notation and quaternion algebra, Comput. Methods Biomech. Biomed. Engin. 7 (3) (2004) 159–166.